

# The traditional Chinese medicine formulation Ruanjian Sanjie Decoction regulates the tumor matrix and improves the anti-tumor efficacy of TP-PEG-LPs

Xin-jun Cai<sup>1#</sup>, Zeng Wang<sup>2#</sup>, Ying-ying Xu<sup>1</sup>, Lihong Ye<sup>3</sup>, Jia-wei Cao<sup>1</sup>, Jian-jun Ni<sup>1\*</sup>, Ting-ting Wu<sup>1\*</sup>

<sup>1</sup>Department of pharmacy, ZheJiang Chinese Medicine and Western Medicine Integrated Hospital, 310003, Hangzhou, Zhejiang, People's Republic of China, <sup>2</sup>Department of pharmacy, Zhejiang cancer hospital, Hangzhou, 310022, People's Republic of China, <sup>3</sup>Department of Traditional Chinese Medicine, ZheJiang Chinese Medicine and Western Medicine Integrated Hospital, 310022, People's Republic of China

The Ruanjian Sanjie Decoction (RSD) is a traditional Chinese medicine (TCM) formulation consisting of *Spica Prunellae*, *Pseudobulbus Cremastrae Seu Pleiones*, *Concha Ostreae* and *Semen Coicis*, and widely used as an adjuvant in anti-cancer therapy. The aim of this study was to determine the effects of RSD on the extracellular matrix (ECM) of tumors, and on the efficacy of anti-cancer nano-formulations in a tumor-bearing mouse model. The mice were treated with triptolide encapsulated in PEG-modified liposomes (TP-PEG-LPs), either alone or in combination with RSD. The combination treatment significantly retarded tumor growth relative to the untreated controls, indicating the potent adjuvant effect of RSD in targeted anti-cancer therapy. In addition, RSD also reduced the amount of total collagen and collagen I and increased that of collagen III in the tumor ECM, along with decreasing the expression of the pro-angiogenic VEGF. Finally, even high doses of RSD did not significantly affect the liver and kidney function or body weight, indicating low toxicity.

**Keyword:** Traditional Chinese medicine. Ruanjian Sanjie Decoction. Tumor matrix. Anti-tumor efficacy. Nano-formulations.

## INTRODUCTION

Nano-formulations are a new generation of anti-tumor therapeutics, and include liposome-encapsulated drugs (e.g. Doxil/Caelyx and DaunoXome which are liposomal preparations of doxorubicin and daunorubicin respectively) and nanoparticles (e.g. the paclitaxel albumin nanoparticle preparation Abraxane) (Cortes *et al.*, 2015; Gradishar *et al.*, 2005; O'Brien *et al.*, 2004). These drug-loaded nanosystems accumulate in the perivascular regions of the tumor owing to their size and the abnormal tumor vasculature, a phenomenon known as enhanced permeability and retention or EPR (O'Brien *et al.*, 2004; Matsumura *et al.*, 1986). However, their therapeutic effects

have been largely ineffective in fibrotic tumors like breast and colon cancers, since the small inter-fibrillar spacing in the tumor interstitium restricts the permeability of nano-formulations larger than 10 nm (Mujtaba *et al.*, 2013; Netti *et al.*, 2000). In addition, abnormal extracellular matrix (ECM) formation also limits the entry of nano-formulations into the deeper parts of the tumor through the vasculature. Matrix solubilizers such as relaxin, bacterial collagenase and angiotensin-converting enzyme (ACE) inhibitors have been used to break the collagen network in tumors, but are associated with potential adverse effects like increased risk of tumor progression (relaxin), hypotension (ACE inhibitors) or systemic toxicity (bacterial collagenase) (Netti *et al.*, 2000; Diop-Frimpong *et al.*, 2011; McKee *et al.*, 2006; Kim *et al.*, 2006).

Ruanjian Sanjie Decoction (RSD) is a traditional Chinese medicine (TCM) formulation consisting of *Spica Prunellae*, *Pseudobulbus Cremastrae Seu Pleiones*, *Concha Ostreae* and *Semen Coicis*, and has been traditionally used to treat turbid phlegm caused by blood stagnation. It is

\*Co-Correspondence: Jian-jun Ni. Department of pharmacy, ZheJiang Chinese Medicine and Western Medicine Integrated Hospital, Hangzhou 310003. China. Phone: 0086-0571-56109722. E-mail: nijianjun1970@aliyun.com. Tingting Wu. Department of pharmacy, ZheJiang Chinese Medicine and Western Medicine Integrated Hospital, Hangzhou310003 China. Phone: 0086-0571-56109722. E-mail: 546440781@qq.com

\*Co-first author: Xin-jun Cai, Zeng Wang

also used as an adjuvant in anti-tumor therapy, on account of its ability to “soften” and then gradually “dissipate” the tumors as per TCM principles (Li *et al.*, 2015). Intra-gastric gavage of RSD in tumor bearing rats enhanced 5-FU absorption in the tumors, while inhibiting its spread to healthy tissues, indicating that dissolution of the tumor collagen network is the likely mechanism underlying RSD action (Huang, Huang, Zheng, 2010). We hypothesized therefore that combining RSD with anti-cancer nano-formulations can augment the therapeutic efficacy of the latter. Accordingly, we tested the ability of RSD to weaken the tumor ECM barrier and increase the therapeutic effects of triptolide encapsulated in PEG-modified liposomes (TP-PEG-LPs) in a tumor-bearing mouse model.

## MATERIAL AND METHODS

### Material

Spica Prunellae (*Prunella vulgaris* L), Pseudobulbus Cremastrae Seu Pleiones (*Pleione bulbocodioides* Rolfe), Concha Ostreae (*Ostrea gigas* Thunberg) and Semen Coicis (*Coix lacryma-jobi* L) were purchased from Zhejiang Chinese Medicine University Chinese medicine Pieces Factory. Soy bean phosphatidylcholine (SPC) was bought from Lipoid GmbH (Ludwigshafen, Germany), cholesterol from Sigma-Aldrich (USA), mPEG2000-DSPE from Fangshuo Co. Ltd. (Shanghai, China), and triptolide from Huawei Rui Ke Chemical Co. Ltd. (Beijing, China). The remaining reagents were bought from Huadong Pharmaceutical Co. Ltd. (Hangzhou, China).

### Cell lines and animals

The NIH-3T3 and MDA-MB-231 breast cancer cell lines were provided by the Type Culture Collection of the Chinese Academy of Sciences (Shanghai, China). Eight-weeks old female SPF-grade BALB/c nude mice weighing ~20 g were purchased from Zhejiang University Animal Laboratory. The animals were acclimatized for 7 days in an environmentally controlled room with temperature 20~26 °C and relative humidity 40%~70% under a 12 h light/dark cycle. Food and water were provided ad libitum. All procedures related to animal handling and care were conducted in accordance to the institutional and governmental protocols.

### Preparation of TP-PEG-LPs and RSD

TP-PEG-LPs were prepared using the thin-film hydration method as described previously (Cai *et al.*,

2015). Briefly, triptolide, cholesterol, lecithin and DSPE-PEG2000 were dissolved in 10 mL chloroform in a 500 mL round bottomed flask, and evaporated in a water bath at 40 °C for 40 min with constant rotation (90 rpm) to remove the chloroform. The resulting solution was then vacuumed for 60 min till a uniform lipid film was formed on the flask wall. The flask was rinsed with PBS, and warmed in a water bath at 40 °C for 40 min (with constant rotation at 90 rpm). The liposome solution was stirred in a magnetic field for 30 min at 1000 rpm, and sonicated in an ice bath (1s pulses separated by 1s intervals) to isolate the liposomes.

The RSD formulation was prepared by mixing Spica Prunellae, Pseudobulbus Cremastrae Seu Pleiones, Concha Ostreae and Semen Coicis in the ratio of 10:15:10:30 by weight, in 8 times the volume of cold water. The mixture was soaked for 5 hours, boiled for 30 min and filtered, and the remaining dregs were extracted again with 6 times the amount of water, followed by another round of boiling and filtering. Both filtrates were combined, and condensed to a suitable concentration, measured as the total decoction mass/final solution volume, in a rotary evaporator. Low-dose, medium-dose and high-dose RSD formulations were prepared by diluting the concentrated mix to 0.75 g/mL, 1.5 g/mL and 3 g/mL respectively.

### Establishment of tumor model and treatment regimen

The MDA-MB-231 and NIH3T3 lines were cultured at 37 °C under 5% CO<sub>2</sub>, harvested, and combined in the ratio of 1:2 to the final density of 7.5\*10<sup>6</sup>/mL (2.5\*10<sup>6</sup> NIH3T3 and 5\*10<sup>6</sup> MDA-MB-231 cells). The nude mice were each subcutaneously injected with 1x10<sup>7</sup> cells in their left hind limbs, and once the tumor volumes reached 60-100 mm<sup>3</sup>, were randomized into the following groups (n = 6 each) based on the 17-day treatment regimens: 1) control group received intra-gastric gavage of physiological saline for the entire duration, 2) TP-PEG-LP group received saline gavage for the first 7 days, followed by daily intravenous injections of 0.05 mg/kg TP-PEG-LPs for 10 days, and the 3) low-dose RSD + TP-PEG-LPs, 4) medium dose RSD + TP-PEG-LPs and 5) high-dose RSD + TP-PEG-LPs groups were given daily intra-gastric gavages of 0.75 g/100g, 1.5 g/100g and 3 g/100g RSD respectively for the first 7 days, followed by 0.05 mg/kg TP-PEG-LPs and (same dose) RSD decoction daily for 10 days.

The body weight of the mice and tumor size were measured on alternate days. On day 18 of the regimen, the mice were sacrificed and the tumors were dissected. The tumor tissues were weighed and measured, and the tumor

volume (V) was calculated as  $V \text{ (cm}^3\text{)} = 1/2ab^2$ , where a is the longest diameter and b is the shortest diameter. The relative tumor volume (RTV) was calculated as  $V_t/V_0$ , where  $V_0$  is the pre-treatment tumor volume and  $V_t$  is the tumor volume measured after each drug dosage. The relative tumor proliferation rate (T/C) was calculated as  $RTV_t/RTV_c \times 100\%$  where  $RTV_t$  is the average RTV of the drug-administered group and  $RTV_c$  is the mean RTV of the model control group. The percentage of tumor weight inhibition (TWI%) was determined according to the following formula:

$$TWI\% = \left[ 1 - \frac{\text{mean tumor weight of treated mice}}{\text{mean tumor weight of controls}} \right] \times 100\%$$

According to the “Guidelines for Non-Clinical Research Techniques of Cytotoxic Antitumor Drugs” by the SFDA, the drug efficacy was evaluated as ineffective when T/C value was  $>40\%$ , and effective when T/C was  $\leq 40\%$  with  $V_t$  or RTV significantly lower compared to that of the control group ( $p < 0.05$ ), or when TWI% was  $\geq 40\%$  and the difference between the tumor weights of the treatment and control groups was significant compared to that of the control group ( $P < 0.05$ ).

### Immunohistochemistry

Tumor tissues were fixed in 10% buffered formalin and embedded in paraffin. The 15  $\mu\text{m}$ -thick tissue sections were dewaxed with xylene, dehydrated through an ethanol gradient, and stained with anti-VEGF, anti-collagen type I and anti-collagen type III antibodies according to standard protocols. The staining intensity or cumulative optical density (IOD) of each sample was evaluated using the Image-Pro Plus 6.0 software, and the percentage IOD relative to tissue area (IOD/Area\*100%) was calculated.

### Measurement of total collagen content

The tumor tissues were processed as described above, and the sections were stained with 0.1% solid green and 0.1% Sirius red in a saturated aqueous picric acid solution at room temperature for 30 mins. The slides were washed repeatedly with distilled water until the excess dyes were completely removed. The stained sections were then scraped off from the slides with a knife, and each sample was dissolved in 150  $\mu\text{L}$  of 0.05 M aqueous NaOH and 50% methanol solution with gentle shaking. The absorbance (OD) of the eluents were measured at 540 nm (Sirius red) and 605 nm (solid green) after M5 enzyme labeling, and the collagen content was calculated as follows:

Non-collagen protein (mg) =  $OD_{605\text{nm}} / 2.08$

Collagen ( $\mu\text{g}$ ) =  $[OD_{540\text{nm}} - 0.26 \times OD_{605\text{nm}}] / 38.4$

Total collagen content ( $\mu\text{g}/\text{mg}$  protein) =  $\text{collagen } (\mu\text{g}) / \text{collagen } (\mu\text{g}) + \text{non-collagen protein (mg)}$

### Scanning electron microscopy (SEM) of tumor ECM

The tumor tissues were fixed with 1% citric acid in 0.1 mM phosphate buffer for 2 hours, rinsed again with the buffer, and then dehydrated through an ethanol gradient. After drying to a critical point, the tissue surfaces were vacuum coated with platinum for 10 min using a coating instrument. The ultrastructure of the tumor matrix and stroma were observed using the SEM.

### Toxicity evaluation

To evaluate drug toxicity, the main indicators of liver and renal functions were measured at the end of the dosing cycle, and the body weight of the mice was regularly monitored during the entire treatment period.

### Statistical analysis

SPSS 22.0 program was used for all statistical analysis. After assessing the normality of distribution, the data were suitably analyzed using the non-parametric Mann-Whitney test or Student's t test. A P value  $< 0.05$  was considered statistically significant.

## RESULTS

### RSD enhances the anti-tumor effects of TP-PEG-LPs

Compared to the untreated control group, the tumor-bearing mice in all treatment groups showed significantly less tumor growth in terms of both weight and volume ( $p < 0.05$  or  $P < 0.01$ ). Furthermore, inclusion of RSD further augmented the tumor inhibitory effects of TP-PEG-LPs in a dose-dependent manner ( $P < 0.05$  or  $P < 0.01$ ) (Figure 1 and Table I). In addition, combination of all doses of RSD with TP-PEG-LPs achieved  $> 40\%$  TWI, with high-dose RSD showing the maximum inhibitory effects. Although TP-PEG-LPs alone decreased the tumor volume, RTV and tumor weight compared to the control group, the T/C was  $> 40\%$  and TWI  $< 40\%$  after the last administration, indicating overall poor anti-tumor efficacy. Inclusion of RSD significantly improved the above parameters ( $P < 0.05$  or  $P < 0.01$ ). In addition, although RSD exerted its effects in a dose-dependent manner, no significant differences

were seen between the different dose-administered groups ( $P>0.05$ ). Taken together, RSD significantly augmented the anti-tumor action of TP-PEG-LPs.

### RSD decreases total collagen content and differentially modulates collagen I and III in the tumor matrix

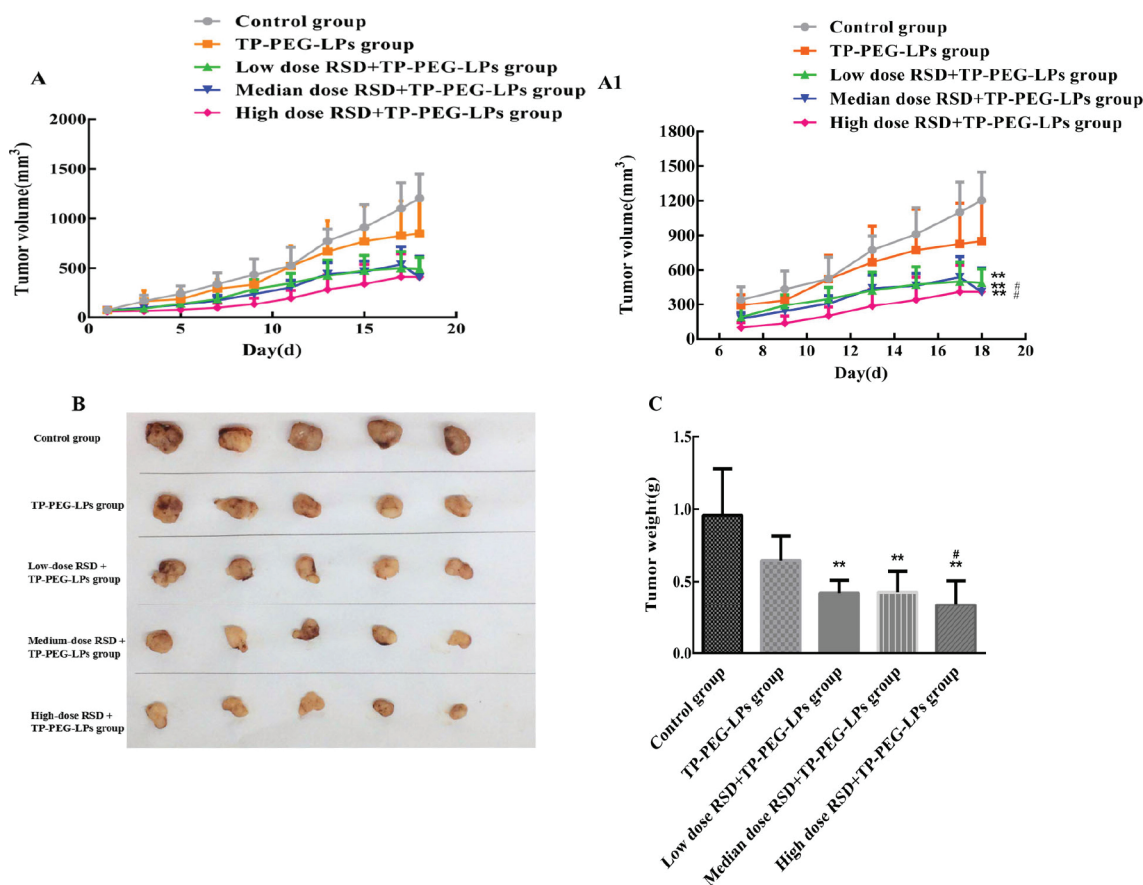
The total and relative (to the total tissue protein) collagen content of tumors were highest in the untreated controls, and both significantly decreased in the RSD-treated groups in a dose dependent manner (Figure 2). In addition, RSD significantly decreased the content of collagen I, which is known to promote tumor proliferation and invasion, in a dose-dependent manner ( $P<0.05$ ; Figure 3 and Table II). In contrast, the lowest amount of the anti-metastatic collagen III was seen in the untreated controls, which increased only slightly in the TP-PEG-LPs group ( $P>0.05$ ) but significantly with the addition of RSD ( $P<0.05$ ), albeit not in a dose-dependent manner (Figure 4).

### RSD disrupts tumor matrix morphology and angiogenesis

SEM indicated dense collagen fibers in the untreated as well as the TP-PEG-LPs-treated tumors, and inclusion of RSD significantly disintegrated the collagen fibers in a dose-dependent manner (Figure 5). VEGF, a pro-angiogenic factor that is frequently overexpressed in tumors and is a target of various anti-tumor drugs, was only slightly reduced by TP-PEG-LPs alone ( $P>0.05$ ). However, addition of RSD led to a significant reduction in VEGF levels ( $P<0.05$  or  $P<0.01$ ) in a dose independent manner (Figure 6).

### RSD does not adversely affect normal tissues

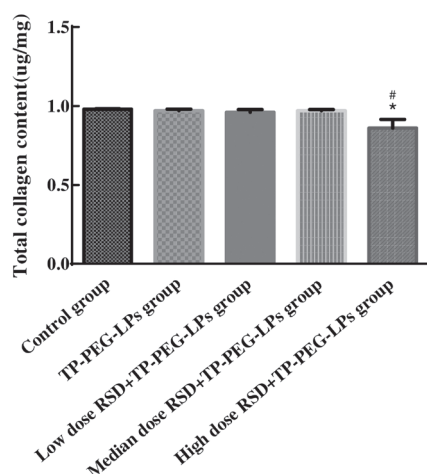
Systemic drug toxicity in the mice was evaluated using routine tests for liver and kidney functions, and by regular monitoring of body weight. The combination of RSD and TP-PEG-LPs did not significantly affect any of these indicators, even at high doses (Figure 7).



**FIGURE 1** A - Tumor growth inhibition (A is the intact figure and A1 is the amplificatory figure.). B - mice were sacrificed and the resected tumors were photographed. C - Tumor weight at the time of sacrifice. Values are expressed as mean $\pm$ SD, n=5. Notice: \*\* $p < 0.01$  vs control group; # $p < 0.05$  vs TP-PEG-LPs.

**TABLE I** - Comparison of proliferation rate (T/C) and tumor inhibition rate in nude mice

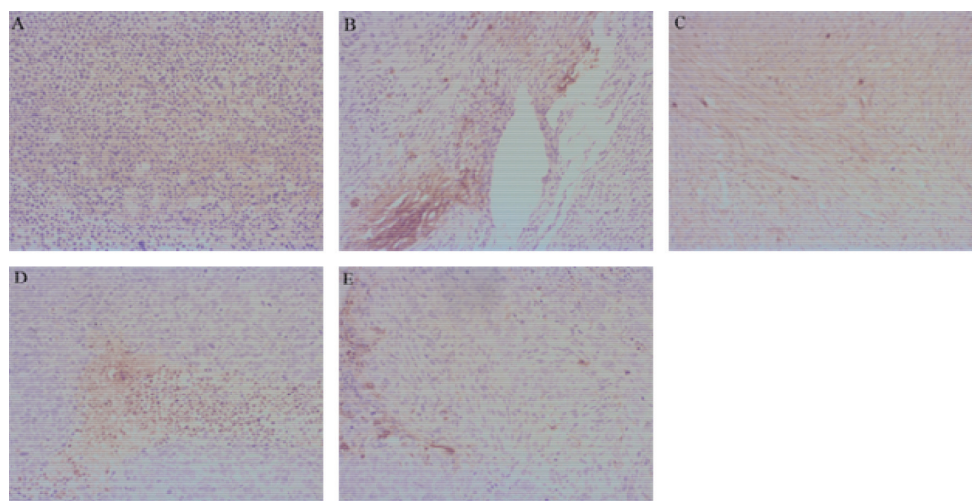
Group	T/C (%)								TWI% (%)
	Day 3	Day 5	Day 7	Day 9	Day 11	Day 13	Day 15	Day 17	
Control group	100	100	100	100	100	100	100	100	/
TP-PEG-LPs group	96.37	77.28	86.03	78.57	99.86	82.62	83.92	74.57	36.92
low-dose RSD with TP-PEG-LPs group	52.82	57.32	54.21	68.17	67.95	53.66	53.56	51.10	60.52
medium-dose RSD with TP-PEG-LPs group	59.36	51.15	51.06	55.22	59.09	56.11	52.07	49.01	59.82
high-dose RSD with TP-PEG-LPs group	47.66	38.52	35.96	39.20	49.59	43.60	44.96	45.55	69.19

**FIGURE 2** - RSD with TP-PEG-LPs differentially modulates total collagen in the tumor matrix. Values are expressed as mean±SD, n=5. Notice: \*\*p < 0.01 vs control group; #p < 0.05 vs TP-PEG-LPs.

## DISCUSSION

Nano-formulations of chemotherapeutic drugs have been in clinical practice for almost two decades, but despite improved tumor targeting and reduced toxicity, have largely shown poor anti-tumor efficacy. In addition to the intrinsic physical and chemical properties of the nano-formulations, several features of the tumor micro-environment like abnormal vasculature, dense ECM, low pH, hypoxia and high interstitial pressure considerably limit the therapeutic efficacy of nano-formulations (Dolor, Szoka, 2018; Glicksman *et al.*, 2017; Goel *et al.*, 2011).

Cancer associated fibroblasts (CAFs) can induce interstitial fibrogenesis, accumulation and cross-linking of ECM proteins, and fibrous bundle formation, all of which harden the tumor texture (Egeblad, Nakasone, Werb, 2010). Myofibroblasts are abundant in breast cancer, and their contraction shrinks and hardens the adjacent tissues

**FIGURE 3** - RSD with TP-PEG-LPs differentially modulates collagen I in the tumor matrix. Tumor sections from each group of animals were immunostained for collagen I. The photographs are representative of sections from 5 tumors/group (×200). (A): Control group; (B): TP-PEG-LPs group; (C): Low-dose RSD with TP-PEG-LPs group; (D): Medium-dose RSD with TP-PEG-LPs group; (E) High-dose RSD with TP-PEG-LPs group. Notice: \*\*p < 0.01 vs control group; #p < 0.05 vs TP-PEG-LPs.

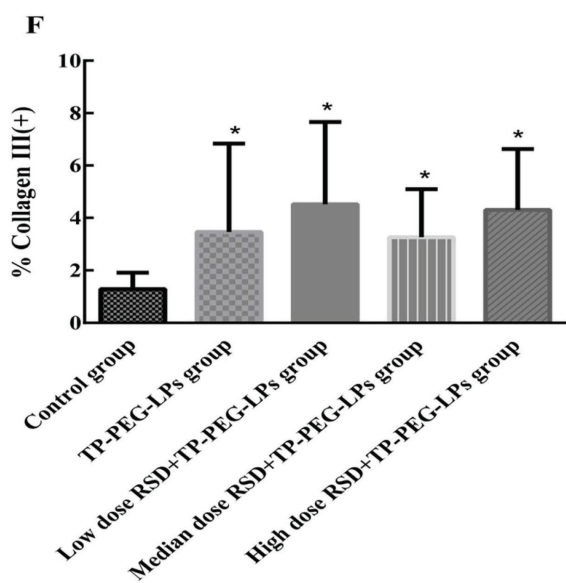
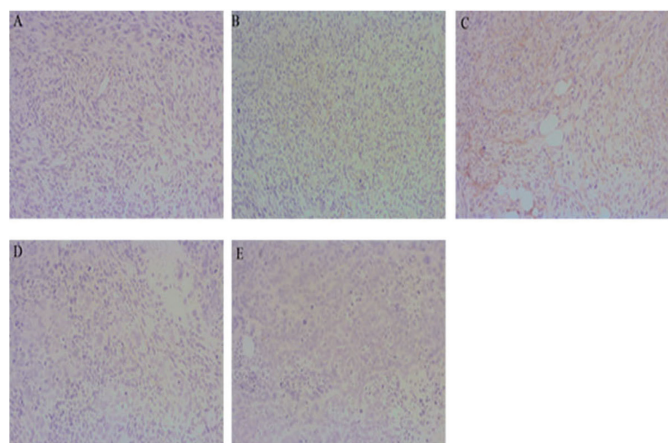


**FIGURE 4** - RSD with TP-PEG-LPs differentially modulates collagen III in the tumor matrix. Tumor sections from each group of animals were immunostained for collagen III. The photographs are representative of sections from 5 tumors/group (×200). (A): Control group; (B): TP-PEG-LPs group; (C): Low-dose RSD with TP-PEG-LPs group; (D): Medium-dose RSD with TP-PEG-LPs group; (E): High-dose RSD with TP-PEG-LPs group. Values are expressed as mean±SD, n=5. (F) Immunohistochemical assay for the collagen III area. Values are expressed as mean±SD, n=5. Notice: \*\*p < 0.01 vs control group; \*p < 0.05 vs TP-PEG-LPs.

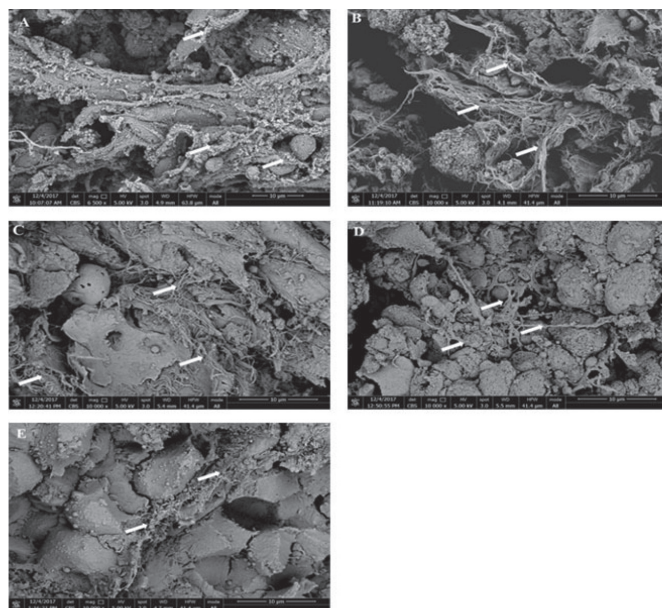


**FIGURE 5** - Scanning electron microscopy (SEM). Representative scanning electron micrographs of collagen fibers of the tumor matrix. The magnification shown is 10000×. (A): Control group; (B): TP-PEG-LPs group; (C): low-dose RSD with TP-PEG-LPs group; (D): medium-dose RSD with TP-PEG-LPs group; (E): high-dose RSD with TP-PEG-LPs group.

(Liu *et al.*, 2016). In addition, CAFs can also promote tumor angiogenesis and provide nutritional support for the tumor cells (Eiro *et al.*, 2018). Therefore, CAFs are an attractive therapeutic target against cancer. Recently, we found that TP-PEG-LPs alone could not significantly inhibit tumor growth, likely due to size restriction and nano-surface modifications. However, their therapeutic effects increased significantly by combining them with RSD, a TCM formulation frequently used to reduce phlegm, soften tumor hardness, increase circulation and remove blood stasis, and strengthen the spleen and stomach. In addition, RSD is also used as an adjuvant in the treatment of various cancers.

TCM formulations like RSD have multiple targets and mechanisms of action, and their therapeutic effects depend on the proportion of individual constituents. Spica Prunellae is the main ingredient of RSD, and

**TABLE II** - Immunohistochemical assay for the collagen I area. Values are expressed as Median(Max,Min), n=5

Group	Collagen I(+)%	Non-parametric statistics (P)
Control group	4.82(11.50,3.16)	
TP-PEG-LPs group	4.14(7.87,0.24)	
Low-dose RSD with TP-PEG-LPs group	4.60(11.25,1.78)	0.014
Medium-dose RSD with TP-PEG-LPs group	4.51(9.44,0.76)	
High-dose RSD with TP-PEG-LPs group	3.70(7.80,0.12)	

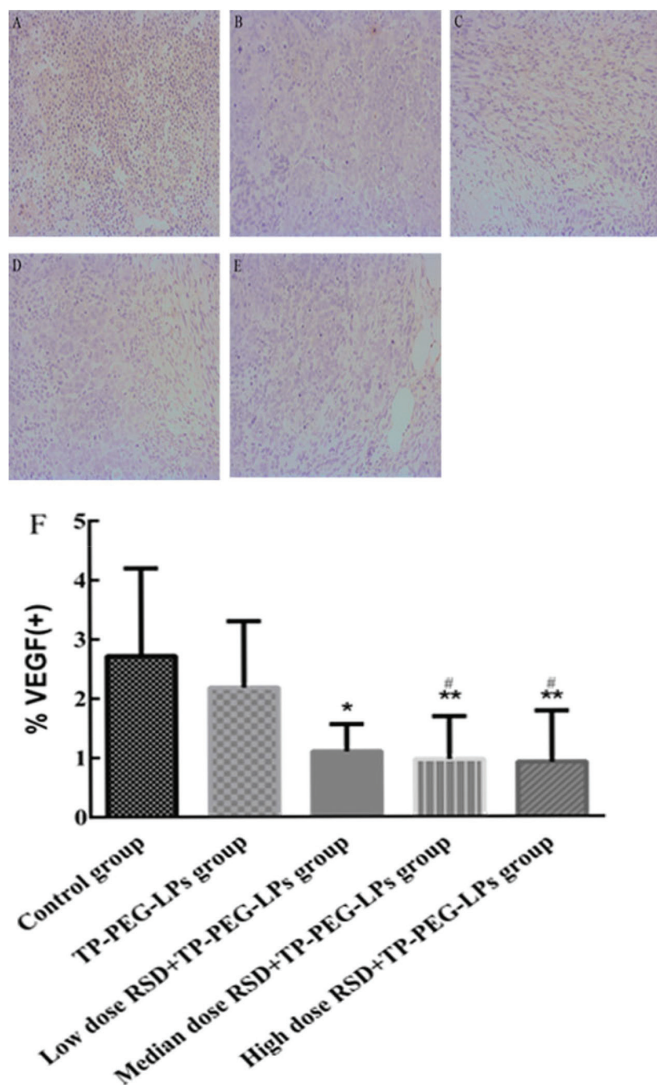


**FIGURE 6** - RSD with TP-PEG-LPs differentially modulates VEGF in the tumor matrix. Tumor sections from each group of animals were immunostained for VEGF. The photographs are representative of sections from 5 tumors/group ( $\times 200$ ). (A): Control group; (B): TP-PEG-LPs group; (C): Low-dose RSD with TP-PEG-LPs group; (D): Medium-dose RSD with TP-PEG-LPs group; (E): High-dose RSD with TP-PEG-LPs group. (F) Immunohistochemical assay for the VEGF area. Values are expressed as mean  $\pm$  SD,  $n=5$ . Notice: \*\* $p < 0.01$  vs control group; # $p < 0.05$  vs TP-PEG-LPs.

accounts for the softening and dispersing effects. Recent studies show that *Spica Prunellae* contains sulfated polysaccharides and triterpenoids, which can reduce the content of hyaluronic acid and collagen, thereby inhibiting connective tissue accumulation and disintegrating the tumor mass (Fang *et al.*, 2005; Itoh *et al.*, 1993). *Pseudobulbus Cremastrae Seu Pleiones* and *Semen Coicis* are known to disperse and dissolve phlegm accumulation, strengthen the spleen and nourish the stomach. *Concha*

*Ostreae* can also dissipate phlegm, and is used to treat phlegm fire and stagnation.

To further explore the mechanism of the action of RSD, we analyzed its effects on various types of collagen. While RSD significantly reduced the total collagen content in tumor tissues, it had variable effects on individual collagen types. High-dose RSD combined with TP-PEG-LPs significantly reduced the content of collagen I, which provides mechanical support to the organs and maintains their structural integrity, thus ensuring normal functioning. In addition, it also promotes tumor cell proliferation, and inhibits the differentiation of macrophages into the anti-tumor  $M_1$  type in order to drive tumor invasion and metastasis (Petrella 2009; Li, Zhou, Guo, Si, 2010). In contrast, the amount of collagen III was lowest in the untreated tumors, and increased significantly following TP-PEG-LPs treatment ( $P < 0.01$ ), independent of RSD ( $P > 0.05$ ). Collagen III was shown to inhibit breast tumor metastasis by inhibiting adhesion, invasion and metastasis (Bagordakis *et al.*, 2016). Both *in vitro* and *in vivo* experiments show that collagen III deficiency promotes tumor cell proliferation and decreases apoptosis (Brisson *et al.*, 2015). Based on these findings, we can surmise that alteration in collagen I and collagen III levels is the likely mechanistic basis of the anti-tumor effects of RSD. Further studies are needed to validate this hypothesis.

Aberrant tumor vasculature is another important factor affecting the transport of nano-formulations. Both tumor cells and mesenchymal cells often have mutations in genes encoding for angiogenic factors, such as VEGF (Ma *et al.*, 2011). The constitutive activation of VEGF results in curved and “leaky” tumor blood vessels, which promote extravasation of nano-formulations, a phenomenon known as EPR (Matsumura, Maeda, 1986). However, the EPR effect also leads to liquid overflow, resulting in increased tumor interstitial pressure and fluid viscosity, ultimately hindering the transport of nano-formulations and the treatment outcomes (Rofstad, Galappathi, Mathiesen, 2014). Furthermore, unrestricted tumor growth and abnormal ECM further compress the blood vessels, which can block blood flow and cause vascular rupture (You, Stallcup, 2017). While TP-PEG-LPs alone had minimal effect on tumor VEGF levels ( $P > 0.05$ ), addition of RSD significantly reduced its expression ( $P < 0.05$ ), indicating that TP itself may not inhibit tumor angiogenesis. It remains to be elucidated whether RSD affects the tumor vasculature directly or indirectly through ECM disruption.

Relatively few studies have correlated the inhibition of tumor angiogenesis with poor delivery of nano-

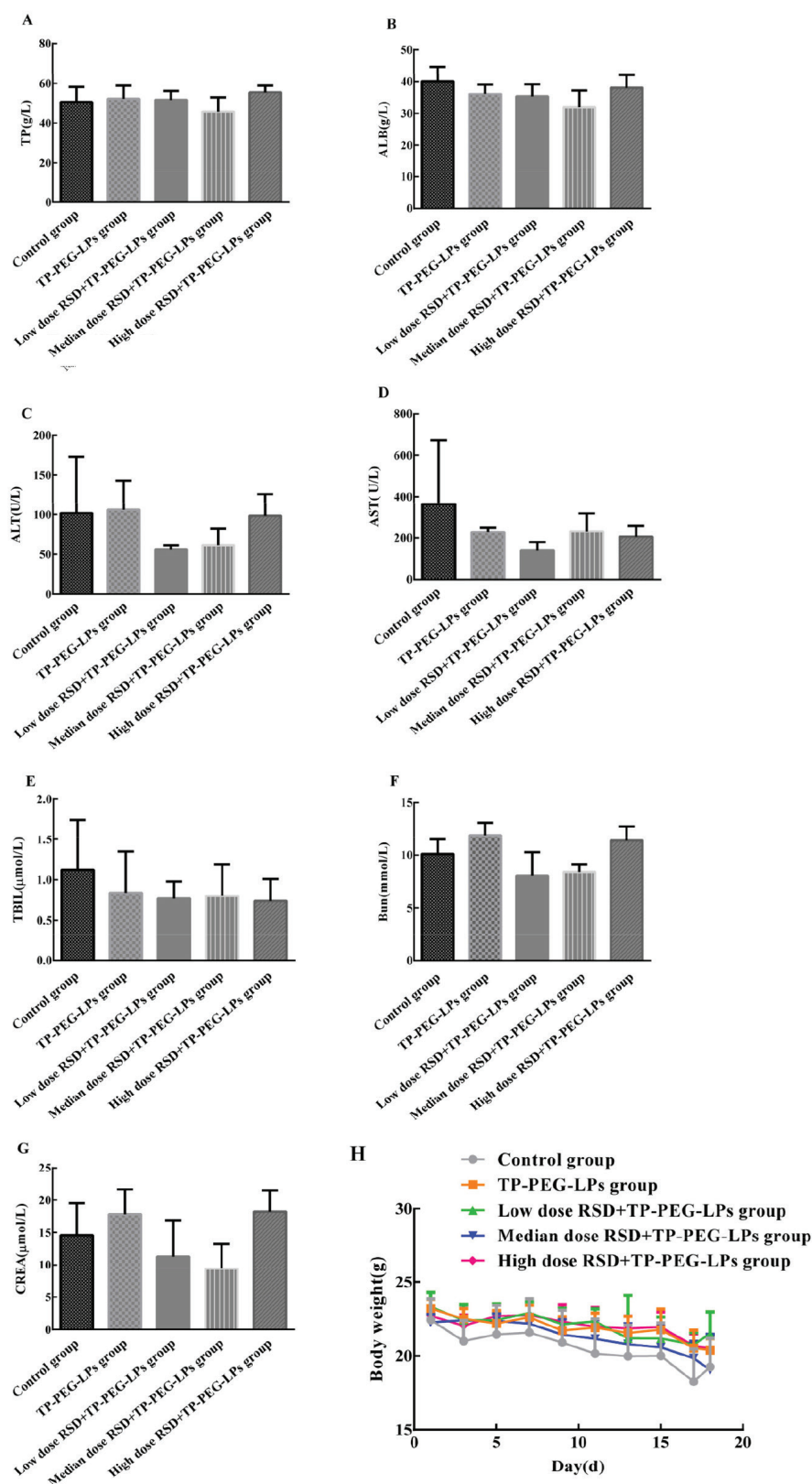


**FIGURE 7** - Systemic drug toxicity in the BALB/C nude mice was evaluated using routine tests for liver and kidney, and by regular monitoring of body weight. (A-E): Liver function of the BALB/C nude mice; (F-G): Kidney function of the BALB/C nude mice; (H): Graph of nude mice weight change in the experimental period. Values are expressed as mean  $\pm$  SD, n=5. Notice: \*\*p < 0.01 vs control group; #p < 0.05 vs TP-PEG-LPs.



formulations to the tumor sites. One study recommended “normalization of tumor blood vessels” as a means to reduce the EPR effect in order to optimize targeted drug delivery (Goel *et al.*, 2011). However, this hypothesis contradicts our findings, and needs to be explored further. Another proposed strategy to enhance the intra-tumor diffusion of nano-formulations is to weaken the tumor ECM, but this may increase the risk of metastasis and recurrence.

In conclusion, RSD significantly enhanced the anti-tumor effects of TP-PEG-LPs in dose-dependent manner, most likely by disrupting the collagen framework of tumor ECM and inhibiting the pro-angiogenic VEGF, without any systemic toxicity. RSD has been used in traditional Chinese medicine for nearly a thousand years and has a good therapeutic effect. Our findings show the potential of RSD as an adjuvant in anti-tumor therapy, and lay a strong foundation for future clinical trials.

## ACKNOWLEDGEMENT

This work was supported by the Chinese medicine science and technology plan of Zhejiang Province (NO 2015ZA148, 2017ZA109) and the Natural Science Foundation of Zhejiang Province (NO Q18H290004, NO YY18H300008), Hospital pharmacy research program of Zhejiang pharmaceutical association, No 2017ZYY16, Hangzhou city science and technology project planning (2015YD21), Science and technology plan of Hangzhou Red Cross Hospital, (NO hhyn201505), Talent Training Program of Zhejiang Cancer Hospital.

## CONFLICTS OF INTEREST

The authors declare no conflict of interest.

## REFERENCES

Bagordakis E, Sawazaki-Calone I, Macedo CC, Carnielli CM, de Oliveira CE, Rodrigues PC, et al. Secretome profiling of oral squamous cell carcinoma-associated fibroblasts reveals organization and disassembly of extracellular matrix and collagen metabolic process signatures. *Tumour Biol.* 2016;37(7):9045-9057.

Brisson BK, Mauldin EA, Lei W, Vogel LK, Power AM, Lo A, et al. Type III Collagen Directs Stromal Organization and Limits Metastasis in a Murine Model of Breast Cancer. *Am J Pathol.* 2015;185(5):1471-1486.

Cai XJ, Wang Z, Wang CY, Zhou HJ, Ni JJ, Xu YY, et al. In Vitro and In Vivo Evaluation of Cationic Liposomes Containing Zoledronic Acid as Anticancer Agent. *Lat Am J Pharm.* 2015;34(6):1239-1245.

Cortes JE, Goldberg SL, Feldman EJ, Rizzeri DA, Hogge DE, Larson M, et al. Phase II, multicenter, randomized trial of CPX-351 (cytarabine:daunorubicin) liposome injection versus intensive salvage therapy in adults with first relapse AML. *Cancer Letters.* 2015;121(2):234-242.

Diop-Frimpong B, Chauhan VP, Krane S, Boucher Y, Jain RK. Losartan inhibits collagen I synthesis and improves the distribution and efficacy of nanotherapeutics in tumors. *Proc Natl Acad Sci USA.* 2011;108(7):2909-2914.

Dolor A, Szoka FC Jr. Digesting a Path Forward: The Utility of Collagenase Tumor Treatment for Improved Drug Delivery. *Mol Pharm.* 2018;15(6):2069-2083.

Egeblad M, Nakasone ES, Werb Z. Tumors as organs: complex tissues that interface with the entire organism. *Dev Cell.* 2010;18(6):884-901.

Eiro N, González L, Martínez-Ordoñez A, Fernandez-Garcia B, González LO, Cid S, et al. Cancer-associated fibroblasts affect breast cancer cell gene expression, invasion and angiogenesis. *Cell Oncol (Dordr).* 2018;41(4):369-78.

Fang X, Chang RC, Yuen WH, Zee SY. Immune modulatory effects of *Prunella vulgaris* L. *Int J Mol Med.* 2005;15(3):491-496.

Glicksman R, Chaudary N, Pintilie M, Leung E, Clarke B, Sy K, et al. The predictive value of nadir neutrophil count during treatment of cervical cancer: Interactions with tumor hypoxia and interstitial fluid pressure (IFP). *Clin Transl Radiat Oncol.* 2017;6:15-20.

Goel S, Duda DG, Xu L, Munn LL, Boucher Y, Fukumura D, et al. Normalization of the vasculature for treatment of cancer and other diseases. *Physiol Rev.* 2011;91(3):1071-1121.

Gradishar WJ, Tjulandin S, Davidson N, Shaw H, Desai N, Bhar P, et al. Phase III trial of nanoparticle albumin-bound paclitaxel compared with polyethylated castor oil-based paclitaxel in women with breast cancer. *J Clin Oncol.* 2005;23(31):7794-7803.

- Huang ZL, Huang XY, Zheng Q. Research Advance on Anti-tumor Effects and Mechanisms of Traditional Chinese Medicine. *Medical Recapitulate*. 2010;(3):386-389.
- Itoh H, Noda H, Amano H, Zhuang C, Mizuno T, Ito H. Antitumor activity and immunological properties of marine algal polysaccharides, especially fucoidan, prepared from *Sargassum thunbergii* of Phaeophyceae. *Anticancer Res*. 1993;13(6A):2045-2052.
- Kim JH, Lee YS, Kim H, Huang JH, Yoon AR, Yun CO. Relaxin expression from tumor-targeting adenoviruses and its intratumoral spread, apoptosis induction, and efficacy. *J Natl Cancer Inst*. 2006 98(20):1482-1493.
- Li A, Zhou T, Guo L, Si J. Collagen type I regulates beta-catenin tyrosine phosphorylation and nuclear translocation to promote migration and proliferation of gastric carcinoma cells. *Oncol Rep*. 2010;23(3):1247-1255.
- Li XJ, Liu GT, Zhao XM, Yao Q, Hu RJ. Effect of Ruanjian Sanjie prescription on pharmacokinetic behavior of 5-fluorouracil in rats. *Chinese Journal of Experimental Traditional Medical Formulae*. 2015;21(11):89-92.
- Liu L, Liu L, Yao HH, Zhu ZQ, Ning ZL, Huang Q. Stromal Myofibroblasts Are Associated with Poor Prognosis in Solid Cancers: A Meta-Analysis of Published Studies. *PLoS One*. 2016;11(7):e0159947.
- Ma J, Chen CS, Blute T, Waxman DJ. Antiangiogenesis enhances intratumoral drug retention. *Cancer Res*. 2011;71(7):2675-2685.
- Matsumura Y, Maeda H. A new concept for macromolecular therapeutics in cancer chemotherapy: mechanism of tumoritropic accumulation of proteins and the antitumor agent smancs. *Cancer Res*. 1986;46:6387-6392.
- McKee TD, Grandi P, Mok W, Alexandrakis G, Insin N, Zimmer JP, et al. Degradation of fibrillar collagen in a human melanoma xenograft improves the efficacy of an oncolytic herpes simplex virus vector. *Cancer Res*. 2006;66(5):2509-2013.
- Mujtaba SS, Ni YB, Tsang JY, Chan SK, Yamaguchi R, Tanaka M, et al. Fibrotic focus in breast carcinomas: relationship with prognostic parameters and biomarkers. *Ann Surg Oncol*. 2013;20(9):2842-2849.
- Netti PA, Berk DA, Swartz MA, Grodzinsky AJ, Jain RK. Role of extracellular matrix assembly in interstitial transport in solid tumors. *Cancer Res*. 2000;60(9):2497-2503.
- O'Brien ME, Wigler N, Inbar M, Rosso R, Grischke E, Santoro A, et al. Reduced cardiotoxicity and comparable efficacy in a phase III trial of pegylated liposomal doxorubicin HCl (CAELYX/Doxil) versus conventional doxorubicin for first-line treatment of metastatic breast cancer. *Ann Oncol*. 2004;15(3):440-449.
- Petrella BL. Assessment of local proteolytic milieu as a factor in tumor invasiveness and metastasis formation: in vitro collagen degradation and invasion assays. *Methods Mol Biol*. 2009;511:75-84.
- Rofstad EK, Galappathi K, Mathiesen BS. Tumor interstitial fluid pressure—a link between tumor hypoxia, microvascular density, and lymph node metastasis. *Neoplasia*. 2014;16(7):586-594.
- You WK, Stallcup WB. Localization of VEGF to Vascular ECM Is an Important Aspect of Tumor Angiogenesis. *Cancers (Basel)*. 2017;9(8):pii: E97.

Received for publication on 16<sup>th</sup> October 2017

Accepted for publication on 10<sup>th</sup> July 2018